Astron. Astrophys. 326, 1044–1054 (1997)

ASTRONOMY
AND
ASTROPHYSICS

Photometric versus empirical surface gravities of eclipsing binaries⋆

C. Jordi[1], **I. Ribas**[1], **J. Torra**[1], **and A. Giménez**[2]

[1] Departament d'Astronomia i Meteorologia, Universitat de Barcelona, Avda. Diagonal 647, E-08028 Barcelona, Spain
[2] LAEFF (INTA-CSIC), Apartado 50727, E-28080 Madrid, Spain

Received 18 March 1997 / Accepted 20 May 1997

Abstract. Systematic differences in photometric stellar surface gravity determination are studied by means of the comparison with empirical values derived from detached double-lined eclipsing binaries. Photometric gravities were computed using Moon & Dworetsky (1985) grids based on Kurucz (1979) atmosphere models, and empirical gravities were taken from Andersen (1991). Individual Strömgren colours and β indices of each component of the binary system have to be taken into account to correctly analyze the observed differences. A compilation of data on a sample containing 30 detached double-lined eclipsing binaries with accurate ($\approx$ 1-2%) determination of mass and radius and available $uvbyH_\beta$ photometric data is also presented.

Correction of the differences in terms of $T_{\rm eff}$ and $\log g$ for the range 11000 K $< T_{\rm eff} <$ 20000 K reduces the mean residuals from 0.13 dex to 0.07 dex. For the range 7000 K $< T_{\rm eff} <$ 8500 K, the consideration of metallicity effects by means of $\delta m_\circ$ index improves the accuracy from 0.20 dex to 0.09 dex.

Key words: stars: fundamental parameters – stars: binaries: eclipsing – stars: early-type – stars: late-type

1. Introduction

Photoelectric photometry yields a determination of stellar physical parameters (M_v, $T_{\rm eff}$, $\log g$, $[Fe/H]$) in a more or less straightforward way. Undoubtedly, these parameters are of extreme importance, since they allow masses, radii, luminosities and ages to be estimated, through models of stellar structure and evolution. Their interest for many studies such as galactic structure or galactic evolution is obvious.

The Strömgren-Crawford intermediate-band photometric system is one of the most widely used to compute physical parameters, and several calibrations – grids – (Moon & Dworetsky 1985 (hereafter MD), Lester et al. 1986) which relate the atmosphere model parameters with the colour indices have been built. Grids based on other intermediate-band photometric systems (Geneva, Walraven, Vilnius) also exist. Kurucz (1979) model atmospheres have generally been used to compute synthetic colours, but Kurucz (1991) models are being implemented in new grids despite a significant discontinuity in the models at $T_{\rm eff} \sim 7000$ K (Künzli et al. 1997).

Several papers discussing the reliability of the published grids and the accuracy when normalizing synthetic colours, as well as comparing determinations from different photometric systems, followed the establishment of the grids (North & Kroll 1989, Castelli 1991, Napiwotzky et al. 1993 (hereafter NSW), Smalley & Dworetsky 1993, Balona 1994, Jordi et al. 1994, among others). From these works several discrepancies arose, mainly in the surface gravity determinations of the hottest stars.

Double-lined eclipsing binaries provide the only direct and model-independent determination of stellar surface gravity. As reviewed by Andersen (1991), detached eclipsing binaries with accurate determination ($\approx 1-2\%$) of their stellar masses and radii are able to put constraints on the stellar models.

Based on a sample of detached double-lined eclipsing binaries with accurately measured parameters, we analyze the systematic differences of the photometric $\log g$ determination through the $uvbyH_\beta$ system. For this purpose, an extensive search in the literature was performed, looking for the photometric indices of each component of the eclipsing binary systems included in our sample. Complementary observations of three systems were carried out and are also reported.

2. Photometry

The sample of detached double-lined eclipsing binaries with accurate fundamental parameters was taken from Andersen (1991) with some updatings coming from new analyses or revisions published later (V539 Ara, AR Aur and β Aur) (Clausen 1996, Nordström & Johansen 1994a, Nordström & Johansen 1994b). For this initial sample of 46 systems, we made an extensive search for individual photometric indices in the literature, but Strömgren-Crawford photometry was only available for 27 of

Send offprint requests to: C. Jordi

⋆ Table 5 is also available in electronic form from CDS via anonymous ftp at 130.79.128.5, and by e-mail request to C. Jordi at carme@facjn0.am.ub.es

them. In addition, we carried out an observing run in the Observatorio de Sierra Nevada (OSN) from which we determined the individual indices of 3 more systems. Details of these observations are given in the subsections below.

Although V, $(b-y)$, m_1 and c_1 indices of each component of the system can be obtained by using the joint indices out of eclipse and the luminosity ratio between the components ($L_{\rm B}/L_{\rm A}$) at each bandpass, the poor photon statistics in the H_{β_n} filter makes it difficult to obtain good light curves and luminosity ratios, so, the determination of the individual β indices is not straightforward (Nordström & Johansen 1994a). In order to pay special attention to this question we will separately describe the obtention of individual V, $(b-y)$, m_1 and c_1 indices and of the β index.

2.1. *uvby colours*

Separate V and $(b-y)$, m_1 and c_1 indices of each component for most of the eclipsing binaries in the sample were directly taken from the literature. For PV Pup and RZ Cha the individual indices had not been published, and we computed them from the joint photometry and the luminosity ratios (Vaz & Andersen 1984, Jørgensen & Gyldenkerne 1975). Individual photometry of three systems (YZ Cas, WX Cep and IQ Per) was obtained as a result of an observing run during November 1995 with a multi-channel photoelectric photometer attached to the 90 cm telescope of OSN. These three systems show a total eclipse (the primary in the case of WX Cep and the secondary for both YZ Cas and IQ Per), allowing us to obtain the luminosity ratio between the components at each filter, and in consequence the individual indices, just by observing during the eclipse and outside it (at $0\overset{p}{.}25$ or $0\overset{p}{.}75$). The adopted $uvbyH_\beta$ photometry of the comparison (C) and check (CK) stars used for each binary system can be found in Table 1. This photometry was computed as an average of the measurements at OSN, those taken from Hauck & Mermilliod (1990, hereafter HM) and those resulting from complementary photometric observations carried out by ourselves at the Observatorio Astronómico Nacional (Calar Alto, Almería, Spain) in September 1995. Tables 2 and 3 summarize the results of $uvby$ measurements for programme stars at OSN.

2.2. *β index*

As previously mentioned, the determination of the β index of each component of the system is difficult, mainly because of the narrow bandpass of the H_{β_n} filter, which causes poor quality light curves. For this reason the publications that provide individual V, $(b-y)$, m_1 and c_1 indices do not quote the individual β index.

However, the β index, together with $c_\circ$, is crucial to determine $T_{\rm eff}$ and $\log\ g$ for B, A and F-type stars. Several authors assign the joint β index of the system to each component, in order to bypass the problem of obtaining individual β indices. Nevertheless, this assumption can lead to important errors in $T_{\rm eff}$ and $\log\ g$ which depend on the difference of spectral types between the components of the system, the degree of evolution and the photometric region each component belongs to. Table 4 illustrates, in the case of KW Hya and GG Lup, how several adoptions of photometric indices, specially β, may cause important differences in the obtained $T_{\rm eff}$ and $\log\ g$, depending on spectral type. For KW Hya, the use of individual colour indices and joint β index may yield unreliable values for $\log g$ (near 5.0) and $T_{\rm eff}$ ($T_{\rm eff\,A} < T_{\rm eff\,B}$), and differences between determinations of 0.4 dex in $\log\ g$ and 1200 K in $T_{\rm eff}$. The $(b-y)$ colour excess and the distance (through M_v calibration) are also highly dependent on β, showing important differences depending on the adopted photometric indices. The same comments can be extended to the hotter system GG Lup, except that the colour excess does not depend on β. Significant inconsistencies are found specially in $\log g$, where the B component appears in some cases to be rather more evolved than the A component.

Table 1. $uvbyH_\beta$ photometry of comparison (C) and check (CK) stars of YZ Cas, WX Cep and IQ Per

	YZ Cas		WX Cep		IQ Per	
	C	CK	C	CK	C	CK
HD	4382	5313	213187	212042	24980	25319
SP	B8	A3	A3	A5	A2	A5
V	5.453	8.057	7.980	7.383	8.354	9.279
	±.089	.036	.025	.014	.013	.011
$(b$–$y)$	−.006	.202	.105	.193	.141	.133
	±.003	.012	.004	.003	.004	.003
m_1	.078	.157	.202	.167	.150	.139
	±.003	.005	.004	.007	.001	.006
c_1	.611	.763	.972	.708	.975	1.045
	±.002	.018	.002	.002	.004	.008
β	2.691	2.758	2.878	2.760	2.855	2.897
	±.014	.009	.001	.002	.005	.005

The large error in the V magnitude for C YZ Cas may be due to intrinsic variability of the star, although the colour indices do not show noticeable variations

Table 2. Differential photometry (variable-comparison) at minimum and out of eclipse for the eclipsing binaries observed at OSN in November 1995

System	Phase	ΔV	$\Delta(b$–$y)$	Δm_1	Δc_1	$\Delta\beta$
YZ Cas	$0\overset{p}{.}75$	.224	.029	.105	.440	.199
		±.003	.003	.003	.010	.007
	Min. II	.322	.010	.108	.495	.217
		±.004	.005	.008	.010	.008
WX Cep	$0\overset{p}{.}75$	.926	.200	−.107	.207	.006
		±.003	.005	.004	.006	.004
	Min. I	1.512	.225	−.097	.210	−.010
		±.006	.006	.011	.023	.016
IQ Per	$0\overset{p}{.}75$	−.645	−.071	−.071	−.324	−.094
		±.005	.003	.005	.008	.005
	Min. II	−.488	−.085	−.071	−.340	−.104
		±.002	.002	.005	.010	.006

Table 3. Luminosity ratios ($q = L_B/L_A$) in $uvbyH_{\beta_w}$ bandpasses derived from observations at OSN in November 1995

System	q_u	q_v	q_b	q_y	q_w
YZ Cas	.0985	.0597	.0755	.0945	.0854
	$\pm$.0081	.0059	.0040	.0050	.0060
WX Cep	.8759	.8164	.7555	.7155	.7669
	$\pm$.0363	.0134	.0081	.0111	.0130
IQ Per	.0955	.1262	.1408	.1556	.1376
	$\pm$.0101	.0083	.0042	.0053	.0073

However, the adoption of more realistic β_A and β_B values yields fully compatible parameters for these systems. Thus, it is essential to obtain individual β indices to perform any accurate study of the photometric determination of $T_{\rm eff}$ or log g.

The lack of luminosity ratios can be compensated by assuming two basic hypotheses which take into consideration the central wavelength of the set of filters (Liu 1993):

- The fraction of flux received during the primary eclipse is the same for filters b, H_{β_w} and H_{β_n} (i.e. $x_b = x_w = x_n = x$, $0 \leq x \leq 1$).
- The luminosity ratio in the H_{β_w} filter is the same as in the b filter (i.e. $q_b = q_w = q$).

The first hypothesis assumes that the inhomogeneities in the flux distribution of the stellar surface (limb darkening, chromospheric activity, reflection effects or gravity darkening) have the same structure and relative intensity in the three bands. This hypothesis is reliable since the central wavelength of b, H_{β_w} and H_{β_n} filters are close to each other and, on the other hand, the eclipsing binaries in the sample are detached, without chromospheric activity and with negligible reflection effects. The second hypothesis is based on the proximity of the central wavelength of b and H_{β_w} filters and on a wide enough bandpass to neglect the absorption caused by the H_β line.

Since our observations at OSN were performed in all six Strömgren-Crawford bandpasses, the luminosity ratio for the H_{β_w} filter can be derived from the observed instrumental magnitude during the eclipse and out of it, in the same way as for $uvby$ filters. As shown in Table 3, these observations support the latter hypothesis, since even for the most unfavourable case (YZ Cas), where the spectral types of the components are very different, the determinations of b and H_{β_w} luminosity ratios are almost compatible.

By using the former hypotheses and some basic algebra, it is possible to get the individual β indices, provided we have enough data, i.e. one value of β and b out of eclipse, another value at mid-eclipse (preferably primary eclipse), and the luminosity ratio for the b filter. In this way, we computed individual β indices of 11 systems in the sample. For the remaining 19 systems with $uvby$ photometry, only β values out of eclipse, i.e. joint β, are reported in the literature (for 3 of the systems the β index was taken from HM and assumed to be out of eclipse). Taking into account the significance of having individual β indices, we applied an indirect method to obtain them. Starting from the joint β index we adopted individual β indices in such a way that: the composition of both indices by using the b luminosity ratio retrieved the value of the joint index; the colour excesses for both components from standard relations were compatible with each other; the distances, obtained through M_v calibrations, were also compatible for the components; the $\log g$ values arising from photometric grids were coherent (in general, $\log g_A \leq \log g_B$) and, finally, that the effective temperatures were also consistent with each other (in general, $T_{\rm eff\,A} \geq T_{\rm eff\,B}$).

2.3. The sample

The sample of detached double-lined eclipsing binaries with accurate physical parameters and currently available individual Strömgren-Crawford colour indices is listed in Table 5. 95% of the components in the sample have B, A and F spectral types. Although later spectral types do not usually fulfill the necessary conditions for accurate masses and radii determination, since intrinsic variability and chromospheric activity is a common feature of cool stars, several programs are currently being undertaken (Clausen 1997, Popper 1996) in order to extend Andersen's (1991) list to eclipsing binaries with G and K spectral types. The masses range from 1 to 23 $M_\odot$, 74% of the stars having masses between 1 and 3 $M_\odot$. In relation to the evolutionary state, there is an important observational bias depending on the mass of the components of the system. For well-detached systems, which can provide accurate masses and radii, the larger the mass of the components, the larger the semimajor axis, and consequently the period, have to be, in order to avoid Roche lobe filling. Such an effect decreases the probability of discovery of the system as an eclipsing binary when the mass of the components increases. In short, there are almost no detached, massive and evolved eclipsing binaries in the sample. Particularly, for spectral types between O8 and A0, only χ^2 Hya A lies significantly out of the ZAMS. V451 Oph A and both components of V539 Ara and CV Vel are also slightly evolved, with log $g \simeq 4.0$. AR Aur and GG Lup appear to be very young systems with components just on the ZAMS (Nordström & Johansen 1994a, Andersen et al. 1993). For later spectral types the number of evolved systems increases considerably, the A components of SZ Cen, WX Cep, AI Hya, V1031 Ori and AI Phe being the most evolved ones, with log $g \simeq 3.5$, near the TAMS.

B components of YZ Cas and IQ Per are much fainter than A components, yielding low luminosity ratios and large errors in the photometric colour indices. Due to these errors, these two stars were rejected for further analysis. On the other hand, AI Phe A is a K subgiant with an effective temperature lower than 6000 K and EM Car is a system of O stars hotter than 30000 K. Both effective temperatures are out of the range of validity of the grids to compute $T_{\rm eff}$ and $\log g$ (see Sect. 3), and these three individual stars were also rejected. Finally, two of the systems (VV Pyx, DM Vir) have almost identical components, so they were regarded as only one star. Taking into account these considerations, of 60 individual stars initially selected (30 systems), 53 of them constitute the final sample.

Table 4. Photometric parameters of the eclipsing binaries KW Hya and GG Lup derived from several adoptions of indices: (1) Joint photometry from HM. (2) Individual photometry from Andersen & Vaz (1984) (KW Hya) and Andersen et al. (1993) (GG Lup) but joint β from HM. (3) Intrinsic photometry adopted by Balona (1994) ($\beta_{\rm A} = \beta^{\rm p}_{0.461}$, $\beta_B = \beta^{\rm p}_{0.003}$). (4) This work ($\beta_{\rm A}$ and $\beta_{\rm B}$ computed from $\beta^{\rm p}_{0.25}$ and $\beta_{\rm MinI}$ through the two hypotheses described in the text)

	Cp.	SP	$(b–y)$	V	m_1	c_1	β	$(b–y)_\circ$	$m_\circ$	$c_\circ$	$E(b–y)^{(a)}$	$M_v{}^{(b)}$	ρ (pc)	$T_{\rm eff}{}^{(c)}$ (K)	$\log g^{(c)}$ (cgs)
KW Hya															
(1)	A	A5m	.123	6.106	.232	.827	2.825	.123	.232	.827	−.004	2.31	57	7905	4.19
	B	F0V	.123	6.106	.232	.827	2.825	.123	.232	.827	−.004	2.31	57	7905	4.19
(2)	A	A5m	.105	6.345	.243	.919	2.825	.105	.243	.919	−.016	1.35	99	7900	3.90
	B	F0V	.244	7.867	.210	.490	2.825	.164	.237	.475	.080	5.46	25	8170	4.96
(3)	A	A5m					2.843	.096	.246	.917		1.54	91	8060	4.02
	B	F0V					2.805	.244	.210	.490		5.31	32	7985	4.88
(4)	A	A5m	.105	6.345	.243	.919	2.845	.104	.243	.919	.001	1.58	89	8080	4.03
	B	F0V	.244	7.867	.210	.490	2.702	.244	.210	.490	−.002	3.70	67	6940	4.52
GG Lup															
(1)†	A	B7V	−.049	5.587	.115	.515	2.746	−.058	.118	.513	.009	.13	121	13975	4.22
	B	B9V	−.049	5.587	.115	.515	2.746	−.058	.118	.513	.009	.13	121	13975	4.22
(2)	A	B7V	−.049	5.890	.097	.450	2.746	−.065	.102	.447	.016	.29	127	14670	4.40
	B	B9V	−.019	7.129	.141	.811	2.746	−.038	.147	.807	.019	−.70	353	11700	3.52
(4)	A	B7V	−.049	5.890	.097	.450	2.731	−.065	.102	.447	.016	−.07	150	14795	4.21
	B	B9V	−.019	7.129	.141	.811	2.817	−.038	.147	.807	.019	.70	186	11515	4.17

(a) Crawford (1979), Olsen (1988) (KW Hya); Crawford (1978) (GG Lup). (b) Crawford (1975,1979) (KW Hya); Crawford (1978) (GG Lup). (c) Moon & Dworetsky (1985)

† Also adopted by Balona (1994)

2.4. Errors

As becomes evident from inspection of Table 5, not all publications provide the errors either in the colour indices or in the luminosity ratio. For those cases where errors are supplied, the mean values are: $\overline{\sigma_V} = 0\overset{\rm m}{.}025$, $\overline{\sigma_{(b-y)}} = 0\overset{\rm m}{.}012$, $\overline{\sigma_{m_1}} = 0\overset{\rm m}{.}020$ and $\overline{\sigma_{c_1}} = 0\overset{\rm m}{.}023$. Errors in the β index could only be computed when using the separation through joint β and $\beta_{\rm MinI}$ and when the errors in the luminosity ratio were available, the mean error is $\overline{\sigma_\beta} = 0\overset{\rm m}{.}027$.

The photometric quality of the sample is not uniform, due both to larger errors of B system components (in general less luminous) and to light curves of different accuracy. On the other hand, the morphology itself of each system may affect the stability of the solution obtained through light curve analysis, and, in consequence, the errors of the luminosity ratios.

3. Photometric $\log g$ determination

Stellar atmosphere models allow us to compute, as a function of the wavelength, the flux emitted by a star with given effective temperature, surface gravity, rotational velocity and chemical composition. With the obtained fluxes it is possible to determine synthetic colour indices that can be normalized by using stars with accurate empirical parameters.

The fully line-blanketed Kurucz's (1979) model atmospheres assume LTE and have been computed for $T_{\rm eff}$ ranging from 5500 to 50000 K and surface gravity limited by radiation pressure. Several calibrations based on Kurucz's models, relating $T_{\rm eff}$ and $\log g$ with $c_\circ$ and β Strömgren-Crawford indices for solar metallicity are available in the literature. Balona (1984) formulated a $T_{\rm eff}$ and $\log g$ calibration for hot stars as a quadratic polynomial in $\log f(\beta)$ and $\log f'(c_\circ)$. MD published grids with a validity range between 6000 and 20000 K in $T_{\rm eff}$ and between 2.0 and 4.5 dex in $\log g$. Moon (1985), Castelli (1991) and NSW proposed different algorithms to interpolate MD grids with extensions up to 30000 K. Finally, Lester et al. (1986) published other photometric grids, which can be used by means of Balona's (1994) expressions. The various grids differ on how synthetic colour indices are obtained and on the number and quality of the used standard stars. Based on the same models, North & Nicolet (1990) and Kobi & North (1990) published calibrations relating atmospheric parameters with the Geneva colour indices.

NSW showed that their interpolation on MD grids provide the most compatible results with the observations. It was also shown (Jordi et al. 1994) that this interpolation is consistent with the determinations through the Geneva photometry. Thus, the NSW interpolation applied to MD grids was the adopted in the present work. From several studies (NSW, Smalley & Dworetsky 1993) it can be inferred that $T_{\rm eff}$ interpolation is precise in the range 6000-20000 K, nevertheless, it can be used up to 30000 K with some loss of accuracy. A good surface gravity determination should be restricted to the $T_{\rm eff}$ interval between 7000 and 20000 K.

Kurucz (1991) presented model atmospheres based on new opacity calculations. Smalley & Dworetsky (1994, hereafter SD) provided us with preliminary grids for the $uvbyH_\beta$ system, which we interpolated by means of the NSW algorithm. SD considered several more standard stars when normalizing,

Table 5. $uvbyH_\beta$ photometry, $\log g$ and $T_{\rm eff}$ for the eclipsing binaries in the sample. $\log g$ (emp.): empirical determination from light and radial velocity curve analysis. $\log g$ (MD) & $T_{\rm eff}$ (MD): photometric determination using MD grids and NSW interpolation. $\log g$ (cor.): $\log g$ (MD) corrected by means of Eqs. (2) and (4). Errors in $\log g$ (emp.) can be found in Andersen (1991) and range from 0.007 to 0.025 dex with a mean value of 0.014 dex. Estimated errors in $\log g$ (MD) and $T_{\rm eff}$ (MD) increase from 0.15 to 0.30 dex and from 200 to 1200 K, respectively, when the temperature increases from 6000 to 20000 K

System	Cp.	Sp	V	$(b-y)$	m_1	c_1	β	$\log g$ (emp.)	$\log g$ (MD)	$\log g$ (cor.)	$T_{\rm eff}$ (MD)	Ref.
BW Aqr	A	F7V	10.98 ± .03	.345±.015	.15 ± .03	.45 ± .03	2.641	3.981	4.14		6365	a
BD−16°6074	B	F8V	11.20 .03	.325 .015	.16 .03	.45 .03	2.661	4.075	4.36		6575	
V539 Ara	A	B3V	6.177	−.038	.088	.249	2.655	3.926	3.78	3.98	18545	b
HD161783	B	B3V	6.862	−.032	.090	.285	2.691	4.096	4.21	4.19	17725	†
AR Aur	A	B9V	6.867 .020	−.043 .010	.142 .012	.857 .015	2.860	4.331	4.38	4.40	11005	c
HD34364	B	B9.5V	6.978 .020	−.021 .010	.162 .012	.892 .015	2.864	4.280	4.32	4.35	10815	†
β Aur	A	A1IV	2.617 .031	−.003 .026	.162 .053	1.124 .057	2.893	3.930	3.89		9435	d
HD40183	B	A1IV	2.668 .031	.005 .026	.206 .053	1.121 .057	2.889	3.962	4.10		9310	
GZ CMa	A	A3m	8.54 .03	.077 .010	.193 .020	1.066 .025	2.884	3.989	3.94	3.93	8425	e
HD56429	B	A4V	8.97 .04	.091 .010	.216 .020	1.002 .025	2.878	4.083	4.00	3.97	8365	
EM Car	A	O8V	9.009 .010	.310 .010	−.038 .010	−.089 .010	2.571	3.857				f
HD97484	B	O8V	9.262 .010	.310 .010	−.047 .010	−.076 .010	2.574	3.928				
QX Car	A	B2V	7.28	−.072	.087	.036	2.638	4.140	4.28	4.17	24470	g
HD86118	B	B2V	7.49	−.072	.092	.076	2.641	4.151	4.15	4.14	23100	
YZ Cas	A	A1m	5.775 .089	.004 .006	.186 .009	1.106 .011	2.899±.008	3.995	3.96	4.01	9220	h
HD4161	B	F2V	8.337 .106	.248 .081	.196 .166	.309 .238	2.609 .132	4.309				†
SZ Cen	A	A7V	9.06	.188	.210	.983	2.808	3.486	3.58	3.53	7725	i
HD120359	B	A7V	9.44	.166	.188	1.019	2.828	3.677	3.67	3.66	7920	
WX Cep	A	A5V	9.492 .026	.330 .007	.105 .012	1.182 .023	2.865 .012	3.640	3.65	3.66	8295	h
HD213631	B	A2V	9.855 .031	.271 .022	.080 .036	1.190 .060	2.890 .023	3.939	3.80		8890	†
CW Cep	A	B0.5V	8.35 .04	.333 .010	−.071 .015	.037 .015	2.595	4.059	3.80	4.05	27475	j
HD218066	B	B0.5V	8.60 .04	.339 .010	−.064 .015	.045 .015	2.599	4.092	3.85	4.06	27275	
RS Cha	A	A8V	6.77	.12	.18	.92	2.816 .026	4.047	3.94	3.98	7810	k
HD75747	B	A8V	6.78	.16	.18	.83	2.758 .028	3.961	3.79	3.81	7295	†
RZ Cha	A	F5V	8.774 .015	.314 .016	.149 .027	.480 .027	2.668	3.909	4.29		6625	l
HD93486	B	F5V	8.830 .015	.304 .017	.165 .029	.468 .029	2.668	3.907	4.33		6630	
AI Hya	A	F2m	9.904	.240	.211	.752	2.742	3.584	3.76	3.69	7180	m
BD+0°2259	B	F0V	10.374	.211	.252	.743	2.778	3.850	3.99	3.88	7500	
KW Hya	A	A5m	6.345 .020	.105 .005	.243 .007	.919 .005	2.845 .008	4.079	3.91	3.84	8080	n
HD79193	B	F0V	7.867 .025	.244 .011	.210 .007	.490 .047	2.702 .011	4.270	4.52		6940	†
χ^2 Hya	A	B8V	5.85	−.02	.11	.83	2.764	3.712	3.65	3.79	11565	o
HD96314	B	B8V	7.57	−.01	.11	.84	2.833	4.188	4.23	4.27	11290	†
GG Lup	A	B7V	5.890 .009	−.049 .007	.097 .011	.450 .012	2.731 .017	4.301	4.22	4.21	14795	p
HD135876	B	B9V	7.129 .014	−.019 .019	.141 .032	.811 .036	2.817 .049	4.364	4.17	4.22	11515	†
TZ Men	A	A0V	6.355 .007	−.025 .007	.140 .010	.941 .010	2.855	4.225	4.13	4.19	10675	q
HD39780	B	A8V	8.324 .015	.185 .007	.176 .015	.689 .015	2.753	4.303	4.23	4.25	7295	
UX Men	A	F8V	8.90	.354	.161	.375	2.622	4.272	4.35		6190	r
HD37513	B	F8V	9.07	.364	.174	.375	2.624	4.306	4.37		6210	
V451 Oph	A	B9V	8.30 .05	.084 .010	.083 .020	.940 .020	2.815 .031	4.038	3.88	3.98	10970	s
HD170470	B	A0V	9.08 .05	.103 .010	.109 .020	.992 .020	2.911 .060	4.196	4.44		10410	†
V1031 Ori	A	A6V	6.89 .08	.10 .01	.17 .02	1.13 .03	2.832	3.560	3.53	3.59	7955	t
HD38735	B	A3V	7.35 .02	.05 .01	.16 .02	1.13 .03	2.867	3.850	3.79	3.86	8315	
IQ Per	A	B8V	7.866 .014	.056 .004	.079 .005	.635 .011	2.758 .008	4.208	4.08	4.14	13000	h
HD24909	B	A6V	9.886 .040	.165 .049	.089 .103	.819 .186	2.836 .092	4.323				†
AI Phe	A	K0IV	9.342 .010	.528 .010	.308 .010	.379 .010	2.583	3.596				u
HD6980	B	F7V	9.319 .010	.316 .010	.172 .010	.421 .010	2.628	3.997	4.11		6235	
ζ Phe	A	B6V	4.30 .01	−.07 .02	.13 .03	.49 .03	2.729	4.122	4.07	4.13	14295	v
HD6882	B	B8V	5.68 .01	−.01 .02	.11 .03	.77 .03	2.818	4.309	4.29	4.31	11750	
PV Pup	A	A8V	7.619 .019	.201 .024	.171 .041	.628 .041	2.705 .049	4.257	4.21	4.22	7090	w
HD62863	B	A8V	7.675 .020	.201 .025	.159 .043	.640 .043	2.735 .050	4.278	4.21	4.24	7085	†
VV Pyx	A	A1V	7.517 .008	.016 .006	.156 .010	1.028 .010	2.890	4.089	4.11		9630	x
HD71581	B	A1V	7.517 .008	.016 .006	.156 .010	1.028 .010	2.890	4.088	4.11		9630	
V1647 Sgr	A	A1V	7.672	.022	.163	1.018	2.902	4.253	4.22		9565	y
HD163708	B	A1V	8.060	.057	.182	.979	2.895	4.289	4.26		8970	
V760 Sco	A	B4V	7.58	.155	.029	.373	2.696	4.177	4.11	4.14	16690	z
HD147683	B	B4V	7.94	.162	.027	.410	2.717	4.259	4.27	4.24	15995	
CV Vel	A	B2.5V	7.40 .02	−.067	.100	.269	2.667	4.000	3.88	4.02	17985	aa
HD77464	B	B2.5V	7.49 .02	−.064	.097	.277	2.671	4.023	3.91	4.04	17815	
DM Vir	A	F7V	9.483 .010	.317 .007	.171 .010	.480 .012	2.655	4.109	4.14		6495	ab
HD123423	B	F7V	9.483 .010	.317 .007	.171 .010	.480 .012	2.655	4.111	4.14		6495	

Table 5. (continued) References for the photometry

a. Clausen (1991); b. Clausen (1996); c. Nordström & Johansen (1994a); d. Nordström & Johansen (1994b); e. Popper et al. (1985); f. Andersen & Clausen (1989); g. Andersen et al. (1983); h. This work; i. Grønbech et al. (1977); j. Clausen & Giménez (1991); k. Clausen & Nordström (1980); l. Luminosity ratios from Jørgensen & Gyldenkerne (1975); m. Jørgensen & Grønbech (1978); n. Giménez (1994); o. Clausen & Nordström (1978); p. Andersen et al. (1993); q. Andersen et al. (1987); r. Clausen & Grønbech (1976); s. Clausen et al. (1986); t. Andersen et al. (1990); u. VandenBerg & Hrivnak (1985); v. Clausen et al. (1976); w. Luminosity ratios from: Vaz & Andersen (1984); x. Andersen et al. (1984a); y. Clausen et al. (1977); z. Andersen et al. (1985); aa. Clausen & Grønbech (1977); ab. Andersen et al. (1984b); † $\beta_{\rm A}$ and $\beta_{\rm B}$ computed from joint β and $\beta_{\rm MinI}$

yielding slight differences with MD grids. In any case, new Kurucz models were only implemented in the hot grid (10000-30000 K) because of a significant discontinuity in the iso-log g lines at $T_{\rm eff} \sim 7000$ K, which was later attributed to an error in the ATLAS9 code (Castelli 1996).

Following Strömgren (1966), we classified the stars in our sample in three different regions (early, intermediate and late), based on the position of the emission maximum with regard to Balmer discontinuity, by using the algorithm of Figueras et al. (1991). Of the 53 individual stars in the final sample, 22 belong to the early region, 6 to the intermediate region and 25 to the late region. Dereddening, absolute magnitude, $T_{\rm eff}$ and $\log g$ calibrations use this classification since Strömgren-Crawford photometric indices $c_\circ$ and β are related to different physical parameters depending on the region.

The applied dereddening calibrations can be found in Jordi et al. (1997). For the sample of eclipsing binaries, the calibrations should provide the same value of the colour excess for both components of each system. We found a good agreement even in those cases where the components belong to different photometric regions. The mean difference of colour excess between the A and B components for the whole sample was:

$$\overline{E(b-y)_{\rm A} - E(b-y)_{\rm B}} = 0.002 \pm 0.016$$

and for those 11 systems with β separated by assuming the two hypotheses described in Sect. 2.2:

$$\overline{E(b-y)_{\rm A} - E(b-y)_{\rm B}} = -0.001 \pm 0.013$$

The values of $T_{\rm eff}$ (from MD grids) and $\log g$ (empirical and from MD grids) for the stars in the sample can be found in Table 5.

4. Discussion

The analysis of light and radial velocity curves of detached double-lined eclipsing binaries provides empirical determinations of masses and radii and, therefore, $\log g$ for both components of the system. For the eclipsing binaries in our sample, the errors associated with the empirical $\log g$ range from 0.007 to 0.025 dex with a mean value of 0.014 dex. Photometric determinations of $\log g$ are of much lower accuracy, with associated errors even an order of magnitude higher.

For each photometric region, we performed an analysis of the differences between empirical and photometric determinations of $\log g$. However, the presence of only six stars in the intermediate region makes it difficult to do any statistically significant studies, so we only present the results for the early and late regions.

The r.m.s. of the difference between the photometric (MD) and empirical determinations of $\log g$ is 0.13 dex for the early region and 0.20 dex for the late region. SD grids (also with NSW interpolation) provide a slightly lower r.m.s. of 0.12 dex for the early region, which was the only one where new Kurucz (1991) model atmospheres were implemented.

4.1. Early region

There are a number of publications in the literature dealing with the problem of systematic trends in the determination of surface gravity for hot stars with respect to various parameters, mainly effective temperature. The lack of hot and evolved stars with accurate surface gravity determination influences negatively in the normalization of grids, especially in the zone with low surface gravity.

NSW performed a study of the differences between determinations of $\log g$ coming from fittings to Balmer lines in observed spectra and from photometric calibrations with a sample of 16 stars. They observed a strong systematic trend and proposed the following correction valid for stars with $T_{\rm eff} > 9000$ K:

$$\log g = \log g_{\rm MD} - 2.9406 + 0.7224\ \log T_{\rm eff}$$

Fig. 2 plots the difference between the photometric and empirical $\log\ g$ as a function of $T_{\rm eff}$ for the stars in our sample. No systematic trends are observed in the plot, and it can also be noticed how NSW's correction seems to be too large when applied to the eclipsing binary sample. As pointed out by Jordi et al. (1994), the correction was obtained with stars cooler than 21000 K and only 4 of them had $T_{\rm eff}$ >15000 K, which makes extrapolation above 20000 K uncertain.

Balona (1994) pointed out a substantial disagreement between the photometric surface gravity and a determination of surface gravity through absolute magnitude calibrations and evolutionary models, especially at low $\log\ g$. He suggested that the discrepancy, which was not observed in his sample of eclipsing binaries, could hardly be attributable to evolutionary models but to non-realistic physics of LTE models for the hottest and most evolved stars. The comparison of surface gravity obtained through absolute magnitude calibrations will be dealt with later in this section, but it is worthwhile mentioning that our sample of eclipsing binaries, although it contains only dwarf stars, shows such a discrepancy between photometric and empirical

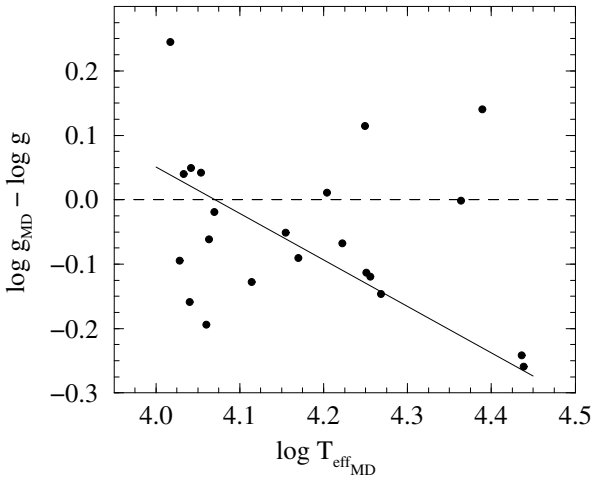

Fig. 1. Differences between photometric and empirical $\log g$ vs. photometric $T_{\rm eff}$ for the stars in the early region. The estimated mean errors are about 0.025 dex in the x coordinate and 0.20 dex in the y coordinate. The straight line stands for the correction proposed by NSW and clearly does not fit the actual residuals

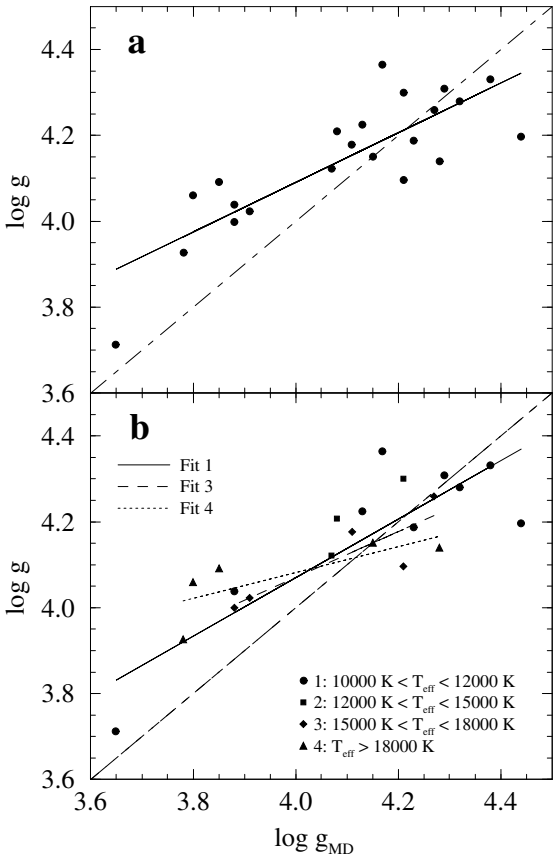

Fig. 2a and b. Comparison of the empirical and photometric $\log g$ determination for the stars in the early region. The long-dashed lines have unit slope. The estimated mean errors are about 0.20 dex in the x coordinate and 0.017 dex in the y coordinate. **a** Linear least squares fit to all points. **b** Separate linear least squares fits to stars in different $T_{\rm eff}$ intervals. Fit 1: 10000 K $< T_{\rm eff} <$ 12000 K, Fit 2: 12000 K $< T_{\rm eff} <$ 15000 K and Fit 4: $T_{\rm eff} >$ 18000 K. Not enough stars in 15000 K $< T_{\rm eff} <$ 18000 K interval

determinations of $\log\ g$, confirming that evolutionary models are not the cause. We can observe the discrepancy because of several new determinations of individual indices compared to Balona (1994), as well as a slightly more extensive sample, and mainly because we consider individual β indices in contrast to the joint β index, which was considered in that work. The discrepancy is clearly shown in Fig. 2a and ba. A linear fit to all stars provides:

$$\log g = (1.779 \pm 0.358) + (0.578 \pm 0.087)\ \log g_{\rm MD} \qquad (1)$$

with a correlation coefficient of $\rho = 0.83$; the mean residuals are reduced from 0.13 to 0.09 dex.

Nevertheless, a more detailed inspection of the plot (Fig. 2a and bb) reveals that a linear regression with zero point and slope depending linearly on effective temperature, could be even more appropriate. A least squares fit supplies the following expression:

$$\log g = (0.425 \pm 0.485)\ +\ (0.913 \pm 0.119)\ \log g_{\rm MD} +$$
$$+ (6.518 \pm 2.108)\,(\log T_{\rm eff} - 4.0) -$$
$$-\ (1.623 \pm 0.522)\,(\log T_{\rm eff} - 4.0)\ \log g_{\rm MD} \qquad (2)$$

with a remarkable $\rho = 0.91$. The mean residual of the fit is 0.07 dex, which means an improvement factor of almost two with respect to the initial dispersion. The validity of the correction should be restricted to the range 11000 K $< T_{\rm eff} <$ 20000 K and $3.5 < \log g < 4.5$, which is the range covered by our sample. The values of the corrected photometric $\log g$ using Eq. (2) can be found in Table 5.

North & Kroll (1989) performed an analysis of the systematic differences in $T_{\rm eff}$ and $\log g$ between the determination through the Geneva photometric system ($\log g_{\rm G}$) and MD grids in Strömgren-Crawford photometric system using Moon's (1985) interpolation ($\log g'_{\rm MD}$). Their sample comprised stars with $T_{\rm eff}$ between 8500 and 25000 K. They observed systematic differences in $T_{\rm eff}$ which vanish when using NSW interpolation (Jordi et al. 1994). However, the differences found in $\log g$, which consist of decreasing slopes when increasing $T_{\rm eff}$, were not removed with the new interpolation algorithm. North & Kroll (1989) gathered stars in different temperature ranges and derived a value for the slope and zero point of a linear fit. We computed a linear fit to the slopes (a) and zero points (b) derived from North & Kroll (1989), quoted in their Table II, as a function of the central effective temperature of the interval for $T_{\rm eff} < 18000$ K. When these values are combined by means of the expression $\log g_{\rm G} = a + b\ \log g'_{\rm MD}$, we obtain:

$$\log g_{\rm G} = 0.764\ +\ 0.833\ \log g'_{\rm MD}\ +\ 6.059\,(\log T_{\rm eff} - 4.0) -$$
$$-\ 1.393\,(\log T_{\rm eff} - 4.0)\ \log g'_{\rm MD} \qquad (3)$$

An inspection of Eqs. (2) and (3) shows that both expressions are perfectly compatible within the errors.

The observed discrepancies in $T_{\rm eff}$ and $\log g$ determination using Kurucz (1979) atmosphere models have been usually attributed to the omission of significant physics for the hotter stars. However, the empirical determinations of $\log g$ through eclipsing binaries allow us to explain some of the discrepancies in a different way. Even though for $T_{\rm eff} > 20000$ K it is well established that LTE atmosphere models do not suitably reproduce the stellar physics, the systematic differences for $T_{\rm eff} < 20000$ K could come not from atmosphere models but from an inaccurate normalization of MD grids. This fact is suggested by the compatibility of Eqs. (2) and (3), and the fact that both Geneva photometric system grids and MD grids are based on the same Kurucz (1979) atmosphere models. In the normalization of MD grids very few hot stars (4 stars with $T_{\rm eff} > 11000$ K) were used as gravity standards and they were in an early evolutionary stage. On the other hand, a more extensive sample of gravity standards (9 stars) and young stars which belong to stellar associations to set ZAMS slope were used in the construction of Geneva grids (North & Nicolet 1990), probably leading to a more accurate normalization. The use of Eq. (2) corrects the $\log g$ values derived through MD grids for systematic effects and provides surface gravities which are compatible with the empirical ones and, additionally, with the determinations from the Geneva photometric system.

The same analysis was carried out by using SD grids, and despite some small changes in $\log g$, the general trends are like those observed in Figs. 2 and 2a and b. A linear regression to correct the discrepancy observed in the equivalent Fig. 2a and ba provides nearly the same value for the slope as that obtained with MD grids. It is worthwhile mentioning that 15 stars with spectrophotometric $\log g$ determination and only 2 eclipsing binary systems, considering joint photometry, were used as gravity standards in the normalization of SD grids.

To end our discussion of the early type stars we will again take up the disagreement pointed out by Balona (1994) when comparing the photometric values of $\log g$ for the early region with those obtained by means of stellar evolutionary models and absolute magnitude calibrations.

To perform the study, we used a sample of 834 stars belonging to the early region (non binary, non peculiar and without emission lines), with Strömgren-Crawford photometry (HM), in the main sequence and with effective temperature between 11000 and 18000 K. From the absolute magnitude of the star, computed from its intrinsic colour indices and by means of a bolometric correction (Schmidt-Kaler 1982), we derived the bolometric magnitude and hence the luminosity. With the latter and the photometric effective temperature obtained from the grids, the interpolation in stellar evolutionary models (we adopted Schaller et al. 1992) provided a value for the surface gravity ($\log g_{\rm ev}$), which was compared with the photometric determination. To avoid possible effects due to the absolute magnitude calibration, we selected different calibrations for the early region: Balona & Shobbrook (1984), Jakobsen (1985) and Crawford (1978). As shown in Fig. 3 the discrepancy between both $\log g$ determinations is clearly observed, regardless of the absolute magnitude calibration. The difference is removed to great extent when the correction given by Eq. (2) is applied. Thus, the discrepancy is no longer observed in the plots with the calibrations of Jakobsen (1985) and Crawford (1978), and only a small trend remains when using the calibration of Balona & Shobbrook (1984).

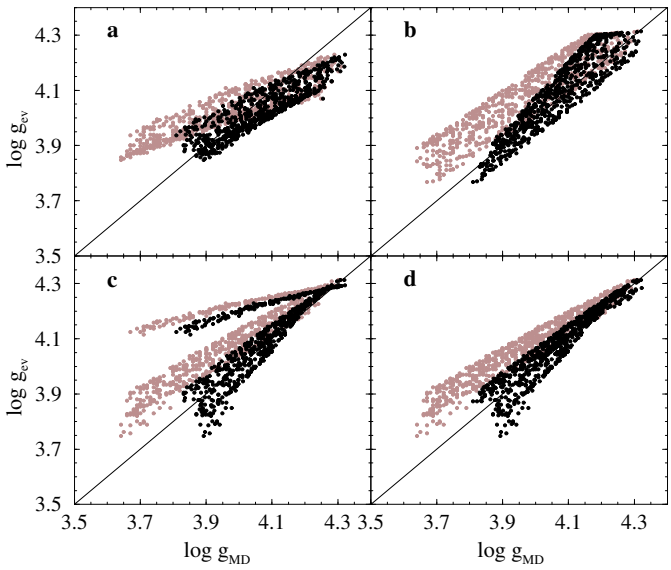

Fig. 3a–d. Comparison of evolutionary (see text) and photometric $\log g$ for 834 stars with 11000 K $< T_{\rm eff} <$ 18000 K. Dark symbols include the correction given by Eq. (2) to the photometric $\log g$ calculation and faint symbols are computed without the correction. The straight line has unit slope. M_v calibration: **a** Balona & Shobbrook (1984), **b** Jakobsen (1985), **c** Crawford (1978), **d** Crawford (1978) with evolutionary factor $-10(\beta_{\rm ZAMS} - \beta)$ for all values of $c_\circ$

The absolute magnitude calibration suggested by Crawford (1978) consists of a table for M_v as a function of β and a correction depending on $\beta_{\rm ZAMS} - \beta$ which accounts for the evolutionary state, with the following expression:

$$M_v = M_v(\beta) - 10\,(\beta_{\rm ZAMS} - \beta) \quad 0.20 < c_\circ \leq 0.75$$
$$M_v = M_v(\beta) \quad c_\circ > 0.75$$

The two trends observed in Fig. 3c arise from the separation into two different zones, in which the evolutionary factor $-10(\beta_{\rm ZAMS} - \beta)$ is applied or not. If the evolutionary factor is used independently of the $c_\circ$ value, the discontinuity disappears, as observed in Fig. 3d, and agreement between $\log g$ determinations is considerably improved.

4.2. Late region

The r.m.s. of the difference between the empirical and the photometric $\log g$ determinations for stars in the late region is 0.20 dex, which appears to be outstandingly high when compared to the early region. Nevertheless, as observed in Fig. 4, stars with $\beta > 2.72$ (i.e. A-type stars, 7000 K $< T_{\rm eff} <$ 8500 K) and those with $\beta < 2.72$ (i.e. F-type stars, 6000 K $< T_{\rm eff} <$ 7000 K) show different behaviours, with mean residuals of 0.18 dex and 0.25 dex, respectively. In fact, the use of

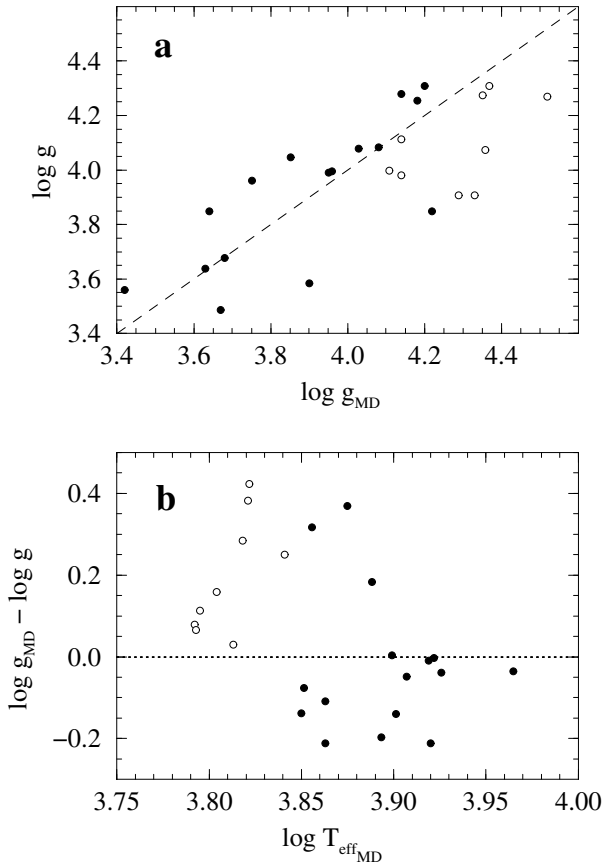

Fig. 4. a Empirical vs. photometric log g for the stars in the late region. The dashed line has unit slope. The estimated mean errors are about 0.15 dex and 0.012 dex in the x and y coordinates, respectively. **b** Differences between photometric and empirical log g as a function of the photometric $T_{\rm eff}$ for the late region. The estimated mean errors are about 0.010 dex in the x coordinate and 0.15 dex in the y coordinate. Filled circles are stars with $\beta > 2.72$ whereas open circles are stars with $\beta < 2.72$

solar metallicity grids (such as MD or SD grids) for a sample of stars with different metallicities will have a negative influence on the achieved precision of the derived parameters and may be the cause of the large scatter.

To test the metallicity effects, we plotted the differences between the photometric and empirical values of log g as a function of $\delta m_\circ$ ($\delta m_\circ = m_\circ$(Hyades)$-m_\circ$(observed)), which is directly related to the metallic abundance in the stellar atmosphere. The plot is shown in Fig. 5. We can distinguish again between two general trends: stars with $\beta > 2.72$ show a clearly defined linear behaviour, whereas stars with $\beta < 2.72$ have a more sparse and scattered distribution.

A linear regression to stars with $\beta > 2.72$ provides the following expression:

$$\log g = \log g_{\rm MD} + (0.03 \pm 0.02) + (5.19 \pm 0.77)\, \delta m_\circ \qquad (4)$$

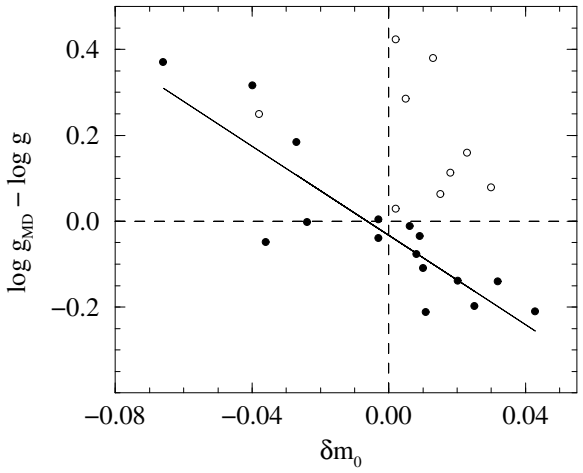

Fig. 5. Differences between photometric and empirical log g vs. δm_0 for the late region. Filled circles are stars with $\beta > 2.72$ whereas open circles are stars with $\beta < 2.72$. A linear least squares fit to the filled circles is represented as a solid line. The estimated mean errors are about 0.02 mag. and 0.15 dex in the x and y coordinates, respectively

with ρ = 0.87. The initial mean residual is reduced to 0.09 dex. This expression was applied to the stars in the sample and the corrected log g values are shown in Table 5.

Dworetsky & Moon (1986) derived an equivalent correction by analyzing the log g of Am stars in open clusters:

$$\log g = \log g_{\rm MD} + 3.442\, \delta m_\circ \quad \text{for } T_{\rm eff} < 8500 \text{ K}$$

with a lower slope than the one derived in this work. Smalley & Dworetsky (1995) studied the same problem by comparing the photometric log g determinations with those computed by means of spectrophotometric flux fits and the metal abundance also derived from the fits. The authors found a clear correlation with $\delta m_\circ$, and, although they did not suggest any explicit correction, the slope in their plots seems to be steeper than in our case.

Finally, stars with $\beta < 2.72$ show a distinct behaviour, not only because the dispersion and the trend are different but because the zero point is not zero. The small number of stars, the poor correlation coefficient and the lack of reliability in the linear regression makes it inadvisable to suggest any correction to the photometric log g determination for this subregion, and moreover, the extrapolation of Eq. (4), obtained for stars with $\beta > 2.72$, makes the residuals even worse. The discrepancy in this region is not likely to be explained by means of normalization problems with the grids, since the number of cool stars, either evolved or not, is presumably enough. Thus, the reason for the discrepancy might be looked for in Kurucz (1979) stellar atmosphere models, which have some problems in accurately describing the surface gravity of stars cooler than 7000 K. Concerning Kurucz (1991) model atmospheres, Künzli et al. (1997) found a sudden change of slope at $T_{\rm eff} \sim 7000$ K when plotting the surface gravity of stars in the Hyades cluster over the cool Geneva grid. This discontinuity was even present after correcting the aforementioned error in the code. Thus, they placed the

inaccuracies of the atmosphere models around the transition between radiative and convective atmospheres and concluded that the surface gravities of cool stars from new Kurucz models are not as reliable as expected, despite the larger number of metallic lines.

5. Conclusions

The systematic differences between photometric and empirical determinations of stellar surface gravity are formulated by means of Eqs. (2) and (4), for stars with 11000 K $< T_{\rm eff} <$ 20000 K and 7000 K $< T_{\rm eff} <$ 8500 K, respectively. These corrections reduce by a factor of two the initial mean residual between both determinations.

For the early region, the discrepancy found between empirical and MD values of $\log g$ had been previously observed when comparing Geneva and MD determinations of $\log g$, which are both based on the same Kurucz (1979) model atmospheres, and so it may be attributable to inaccuracies when normalizing the grids. The inaccuracies may be due to the small number of hot stars used. MD grids with NSW interpolation algorithm and the correction obtained in this work (Eq. (2)) provide $\log g$ photometric determinations with an accuracy of 0.07 dex.

For the late region, the correction, in terms of $\delta m_\circ$, is a way of correcting the inaccuracy introduced when using solar metallicity grids for stars with different metallicities. In this case, the initial mean residual is reduced to 0.09 dex.

Stars with intermediate effective temperatures (8500 K $< T_{\rm eff} <$ 11000 K) could not be studied due to the lack of stars in our sample belonging to this range. On the other hand, stars with $T_{\rm eff} <$ 7000 K present large discrepancies that cannot be explained in terms of metallicity effects or inaccuracies in the normalization of the grids. Problems in the input physics of the model atmospheres can be the cause of such discrepancies but a larger sample of eclipsing binaries or more work with new models is needed to correctly formulate the cause.

Grids based on more recent stellar atmospheres (Kurucz 1991) yielded similar dispersions and systematics in the early region and, in spite of the unavailability of $uvbyH_\beta$ grids, some studies in Geneva photometric system reveal unsolved discontinuities in the surface gravity of the late region.

At the moment, our sample contains 30 detached double-lined eclipsing binaries with accurate ($\approx$ 1-2%) determination of mass and radius and available individual $uvbyH_\beta$ photometry for each component of the system. More observations are planned to enlarge the present sample.

Finally, the use of the individual photometric colours and β indices for each component of the eclipsing binary system has proved to be essential to derive the above-mentioned corrections. The observed trends are not so evident when using the joint β index for both components of the system, since the additional scatter hides systematic behaviour.

Acknowledgements. J.M. García is thanked for his kind collaboration when performing and reducing the observations at OSN. This work was supported by the Spanish CICYT under contract ESP95-0180. I.R. also acknowledges the grant of the *Beques predoctorals per a la formació de personal investigador* by the CIRIT (Generalitat de Catalunya)(ref. FI-PG/95-1.111). The 90 cm telescope is operated by the Instituto de Astrofísica de Andalucía in the Observatorio de Sierra Nevada (Granada, Spain).

References

Andersen, J., 1991, A&AR 3, 91
Andersen, J., Clausen, J.V., 1989, A&A 213, 183
Andersen, J., Clausen, J.V., Nordström, B., Reipurth, B., 1983, A&A 121, 271
Andersen, J., Clausen, J.V., Nordström, B., 1984a, A&A 134, 147
Andersen, J., Clausen, J.V., Nordström, B., 1984b, A&A 137, 281
Andersen, J., Clausen, J.V., Nordström, B., Popper, D.M., 1985, A&A 151, 329
Andersen, J., Clausen, J.V., Nordström, B., 1987, A&A 175, 60
Andersen, J., Clausen, J.V., Nordström, B., 1990, A&A 228, 365
Andersen, J., Clausen, J.V., Giménez, A., 1993, A&A 277, 439
Andersen, J., Vaz, L.P.R., 1984, A&A 130, 102
Balona, L.A., 1984, MNRAS 211, 973
Balona, L.A., 1994, MNRAS 268, 119
Balona, L.A., Shobbrook, R.R., 1984, MNRAS 211, 375
Castelli, F., 1991, A&A 251, 106
Castelli, F., 1996, in: Model Atmospheres and Spectrum Synthesis, proceedings of the 5th Vienna International Workshop, p. 85
Clausen, J.V., 1991, A&A 246, 397
Clausen, J.V., 1996, A&A 308, 151
Clausen, J.V., 1997, in: Fundamental Stellar Properties: The Interaction between Observation and Theory, proceedings of the Symposium 189 of IAU, (in press)
Clausen, J.V., Giménez, A., 1991, A&A 241, 98
Clausen, J.V., Grønbech, B., 1976, A&A 48, 49
Clausen, J.V., Grønbech, B., 1977, A&A 58, 131
Clausen, J.V., Nordström, B., 1978, A&A 67, 15
Clausen, J.V., Nordström, B., 1980, A&A 83, 339
Clausen, J.V., Gyldenkerne, K., Grønbech, B., 1976, A&A 46, 205
Clausen, J.V., Gyldenkerne, K., Grønbech, B., 1977, A&A 58, 121
Clausen, J.V., Giménez, A., Scarfe, C.D., 1986, A&A 167, 287
Crawford, D.L., 1975, AJ 80, 955
Crawford, D.L., 1978, AJ 83, 48
Crawford, D.L., 1979, AJ 84, 1858
Dworetsky, M.M., Moon, T.T., 1986, MNRAS 220, 787
Figueras, F., Torra, J., Jordi, C., 1991, A&AS 87, 319
Giménez, A., 1994, private communication
Grønbech, B., Gyldenkerne, K., Jørgensen, H.E., 1977, A&A 55, 401
Hauck, B., Mermilliod, M., 1990, A&AS 86, 107 (1992 revision; private communication) (HM)
Jakobsen, A.M., 1985, PhD Thesis, Univ. of Aarhus, Denmark
Jordi, C., Masana, E., Figueras, F., Torra, J., Asiain, R., 1994, Space Sci. Reviews 66, 203
Jordi, C., Masana, E., Figueras, F., Torra, J., 1997, A&AS 123, 83
Jørgensen, H.E., Grønbech, B., 1978, A&A 66, 377
Jørgensen, H.E., Gyldenkerne, K., 1975, A&A 44, 343
Kobi, D., North, P., 1990, A&AS 85, 999
Künzli, M., North, P., Kurucz, R.L., Nicolet, B., 1997, A&AS 122, 51
Kurucz, R.L., 1979, ApJS 40, 1
Kurucz, R.L., 1991, in: Precision Photometry: Astrophysics of the Galaxy, eds. A.G. Davis Philip, A.R. Upgren and K.A. Janes, L. Davis Press, Schenectady, p. 27
Lester, J.B., Gray, R.O., Kurucz, R.L., 1986, ApJS 61, 509
Liu, Q., 1993, A&AS 101, 49

Moon, T.T., 1985, Commun. Univ. London Obs., 78
Moon, T.T., Dworetsky, M.M., 1985, MNRAS 217, 305 (MD)
Napiwotzky, R., Schönberner, D., Wenske, V., 1993, A&A 268, 653 (NSW)
Nordström, B., Johansen, K.T., 1994a, A&A 282, 787
Nordström, B., Johansen, K.T., 1994b, A&A 291, 777
North, P., Kroll, R., 1989, A&AS 78, 325
North, P., Nicolet, B., 1990, A&A 228, 78
Olsen, E.H., 1988, A&A 189, 173
Popper, D.M., 1996, ApJS 106, 133
Popper, D.M., Andersen, J., Clausen, J.V., Nordström, B., 1985, AJ 90, 1324
Schaller, G., Schaerer, D., Meynet, G., Maeder, A., 1992, A&AS 96, 269
Schmidt-Kaler, T., 1982, in Landolt-Börnstein, eds. K. Schaifers and H.H. Voigt, Vol. II, Subvol. B, p. 453
Smalley, B., Dworetsky, M.M., 1993, A&A 271, 515
Smalley, B., Dworetsky, M.M., 1994, private communication (SD)
Smalley, B., Dworetsky, M.M., 1995, A&A 293, 446
Strömgren, B., 1966, ARA&A 4, 433
VandenBerg, D.A., Hrivnak, B.J., 1985, ApJ 291, 270
Vaz, L.P.R., Andersen, J., 1984, A&A 132, 219

This article was processed by the author using Springer-Verlag LaTeX A&A style file *L-AA* version 3.